Studies of buried pipe behaviour

I.D. Moore
GeoEngineering Centre at Queen's – RMC, Queen's University, Kingston, Ontario, Canada

ABSTRACT: The study of shells interacting with particulate and other solids is not confined to investigations focused on silo structures. The mechanical response of buried pipes is governed by the shell's interaction with the surrounding solid, rather than the material contained within. The author's studies over the past decade include projects examining the limit states of flexible and rigid buried pipe undergoing deterioration, as well as pipes installed, replaced, or repaired using trenchless technologies. An overview of these projects demonstrates the variety of issues to explore, and a series of problems in nonlinear mechanics influencing the service load response and stability limits of the pipes and the soil that surrounds them.

1 INTRODUCTION

Buried pipes and conduits provide us with water, gas, electricity, and communications, and remove storm and waste-water from our communities. Though out of sight and largely neglected for decades, the public is now becoming aware of the need for engineers to replace and upgrade our increasingly inadequate pipe infrastructure, Figure 1. Recorded here are examples of the author's research over the past ten years examining the mechanics of buried pipes to develop better understanding of:

i. The stability of deteriorated structures like
   a. Rigid pipes influenced by erosion voids, and
   b. Metal culverts experiencing corrosion;
ii. Pipe repair using polymer liners considering
   a. Buckling under external fluid pressure, and
   b. Bending induced by earth loads;
iii. Pipe replacement using bursting resulting in
   a. Uplift at the ground surface, and
   b. Pulling force and disturbance to adjacent pipes;
iv. Pipe installation using directional drilling where
   a. Axial pipe stress distributions vary with time
   b. Mud pressures are limited to prevent mud loss.

2 DETERIORATED PIPE STRUCTURES

The mechanics of gravity flow sewers and culverts has been well explained in the twentieth century, with contributions on rigid (e.g Marston and Anderson, 1913) and flexible (e.g. Spangler, 1956) structures, and rational analyses developed since the 1960's that explain how pipe stiffness relative to the surrounding ground influences the stability limit states (e.g. Hoeg, 1968). While there might seem little need for further research, the processes by which the stability of pipes change over time are only now being studied (e.g. Tan and Moore, 2007; El Taher and Moore, 2008), considering the roles of pipe deterioration (fractures in rigid structures, Figure 1a, and corrosion of flexible metal structures, Figure 1b), as well as soil erosion. Figure 2a shows an erosion void visible beside a metal culvert, developing after wall perforation. Similar voids develop besides rigid pipe structures (Spasojevic et al., 2006).

Two recent studies are perhaps the first to explore the resulting effects on pipe stability. First, Tan and Moore (2007) used finite element analyses to examine the stresses within a rigid sewer pipe as voids grow at the springline. Figure 2b shows a typical mesh, with three different sized circular zones at the springline modeling the progress of void growth, Figure 2c. The geometrical feature found to dominate tensile bending stresses and pipe fracture at the crown, invert and springlines (Figure 2b) is the angle of void contact α on the external pipe surface (not, for example, the void width). Idealizing the fractured pipe using four quadrants, Figure 3, the analysis was then extended to calculate deformations (decreases in vertical diameter ΔD_V and increases in horizontal diameter ΔD_H), Figure 4.

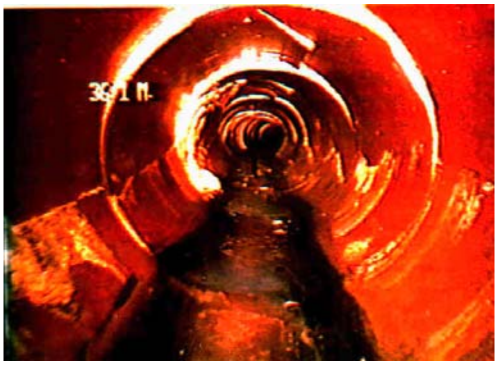

a. Fractured Clay Sewer in Toronto.

b. Corroded metal culvert in Eastern Ontario

Figure 1. Typical damaged structures

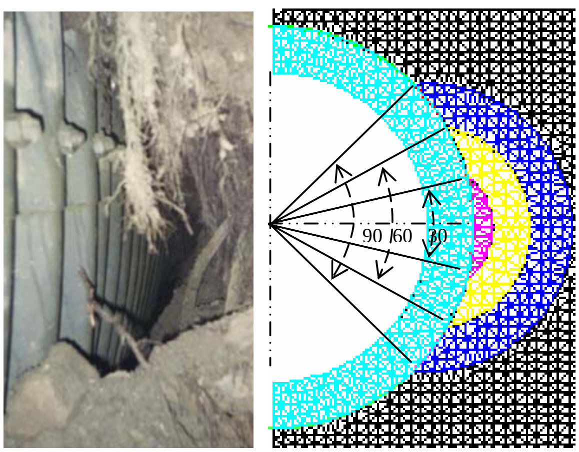

a. Springline void. b. Mesh with void contact angles

Figure 2. Finite element analysis considering erosion voids (after Tan and Moore, 2007).

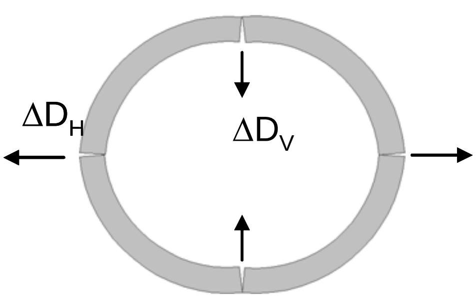

Figure 3. Four segment hinge mechanism for rigid pipe deformation after fracturing (Moore, 2008).

Following comparison with the kinematics of fractured pipe deformation (Law and Moore, 2007), it was found that the fractured pipe responds much like a flexible pipe. Flexible pipe theory can therefore be used to estimate the fractured pipe deformations. For example, a pipe of internal diameter ID_{pipe} and thickness t_{pipe} has ΔD_H given by

$$\Delta D_H / ID_{pipe} \approx 1.6\frac{\sigma_V}{M_S}(1+\frac{2t_{pipe}}{ID_{pipe}}) \qquad [1]$$

where overburden stress σ_v, lateral earth pressure ratio K, constrained modulus M_s and Poisson's ratio of the soil ν_s all influence the response, and the expression 1.6 is based on K =0.45, and ν_s=0.3. Other combinations of K and ν_s result in values ranging from 1.4 to 1.7. The kinematics of pipe deformation can then be used to provide a relationship between changes in vertical and horizontal diameters:

$$\Delta D_V = -\Delta D_H (1-\frac{2.t_{pipe}}{OD_{pipe}}) \qquad [2]$$

for pipe with outer diameter OD_{pipe} Finite element analyses of fractured pipe deformations have also been conducted examining the increase in pipe deformations as erosion voids like those seen in Figure 2b develop at the springlines. These calculations are being used to interpret soil condition from pipe geometry visible in Closed Circuit Television images obtained during sewer inspections, Moore (2008).

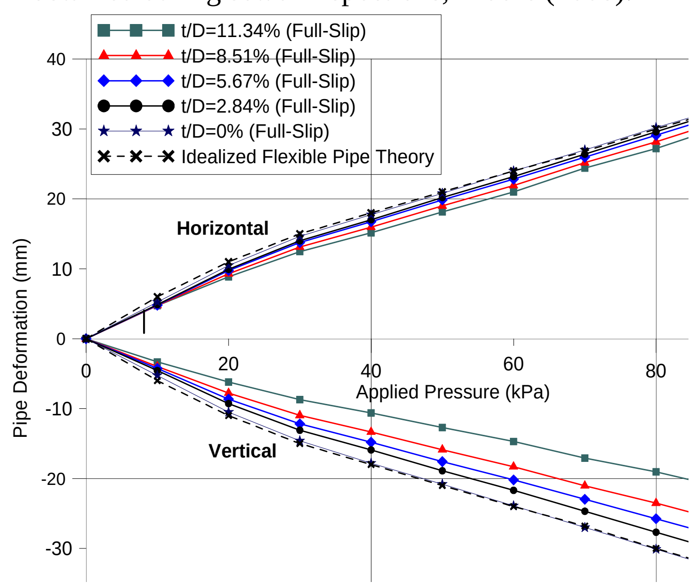

Figure 4. Fractured pipe deformation versus overburden (finite element analysis and flexible pipe theory), Moore (2008).

Finite element studies of corroded metal culvert stability have recently been reported by El Taher and Moore (2008). Corrugated metal culverts of three different diameters have been considered, each composed of 152mm x 52mm corrugated steel plate, Figure 5a. Initial pipe thicknesses satisfy current North American design requirements defined by AASHTO. Reductions in wall thickness are modelled with three different angles of uniform thickness steel loss across the invert, Figure 5b.

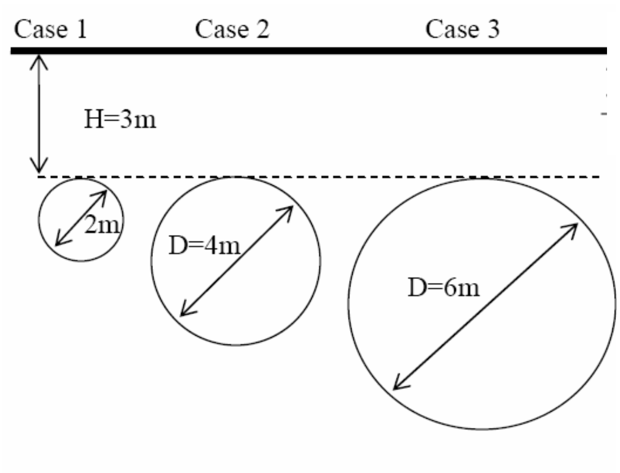

a. Geometry of the circular metal culverts

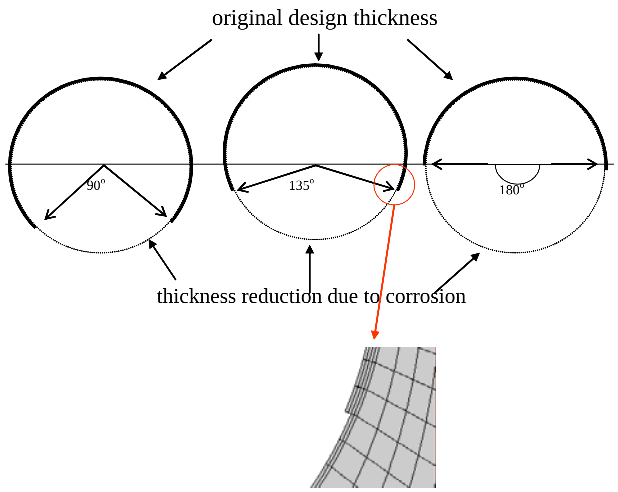

b. Extent of uniform wall loss across the invert

Figure 5. Deteriorated culvert problems considered by El Taher and Moore (2008).

Figure 6 presents changes in factor of safety against yield at the junction between the corroded and uncorroded sections (where thrust in the corroded section is greatest) as a function of the amount of plate thickness that remains. The governing factor of safety is the lesser of this and the factor of safety at the location of maximum thrust (the springline). For all cases considered, the factor of safety just below the junction decreases linearly with wall thickness. This reflects the fact that the hoop thrusts in the structure barely change as the wall corrodes (the culvert is already flexible in bending compared with the surrounding soil and wall loss has no significant effect on arching, i.e. the maximum compressive thrust).

Figure 7 summarizes the effect of corrosion on culvert buckling strength. These indicate that there is little change in resistance to buckling until less than half of the thickness remains. After that point, stability reductions accelerate. As expected, reductions in buckling strength are greater for the case where wall thickness loss extends from springline to springline. However, for these culverts with good soil support, yield is the governing limit state.

Unless the surrounding soil degrades, the increases in structural deformations or decreases in buckling strength that occur are not important. Work is therefore underway to study the effect of soil erosion beside metal culverts (like that in Figure 2a) on metal culvert stability and serviceability.

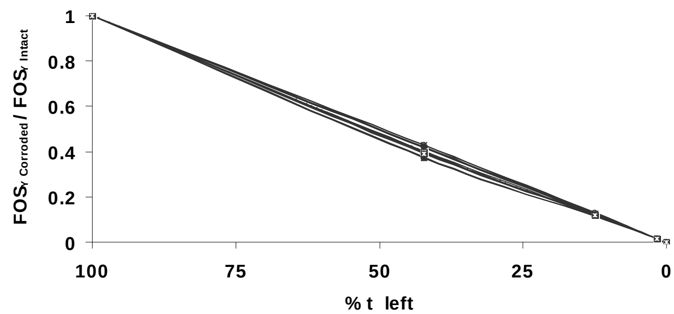

Figure 6. Reduced factor of safety for yield at the top of corroded zone, El Taher and Moore (2008).

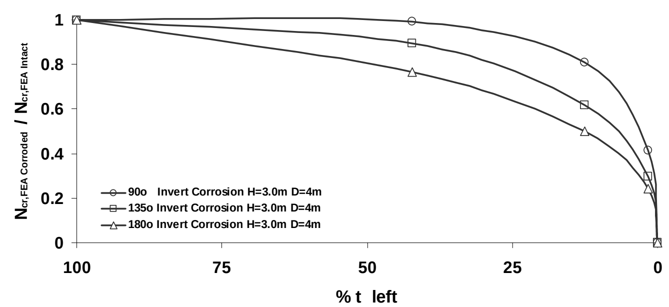

Figure 7. Reduced factor of safety for buckling due to corrosion, El Taher and Moore (2008).

3 SEWER PIPE REPAIRS

3.1 *Liners and their performance limits*

A variety of techniques have been developed to repair buried gravity flow and pressure pipes using polymer liners. Two liner types are illustrated in Figure 8.

Two performance limits need to be considered when designing polymer liners within gravity flow pipes, as illustrated in Figure 9. First, the liner needs to be able to support the external fluid pressures in the surrounding ground without buckling, Figure 9a (Moore and Law, 2006; El Sawy and Moore, 1997). Second, the liner needs to withstand tensile bending strains at crown and invert as the vertical diameter of the fractured sewer decreases under the influence of the earth loading, Figure 9b (Law and Moore, 2003).

a. Clay sewer after repair b. Slip-lining of corroded metal culvert in Northern Ontario.
Figure 8. Damaged pipe repair using liners

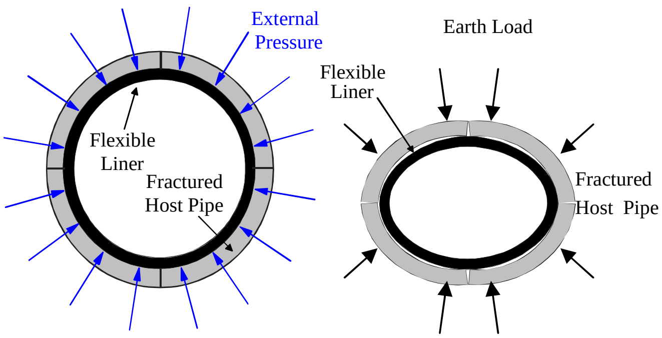

a. External groundwater b. Earth loading
Figure 9. Performance limits for liners within gravity flow sewers, Moore (2008).

3.2 *Measurements of buckling strength, linear, and nonlinear buckling analyses*

Almost at the outset of liner installation to repair damaged sewer pipes, it was understood that external groundwater pressure could lead to buckling of a shell placed within a shell. Experiments by Aggarwal and Cooper (1984) summarized in Figure 10 clearly showed that the critical external water pressure P_{cr} was significantly higher than the value for an unsupported circular shell placed inside that fluid, Levy (1884), over a practical range of diameter to thickness ratios D/t. For the next two decades, an empirical 'enhancement factor' of 7 was used for design, given that this brings the calculated buckling pressures up to the base of the test data (e.g. ASTM F1216-93).

Similar buckling tests performed in North America subsequently raised questions about the scatter in the test data. The buckling of a ring within a ring is a nonlinear phenomenon where the shell has to contract circumferentially before it can buckle. Imperfections become key, and the tests of Aggarwal and Cooper (1984) were influenced by variable sized initial gaps between the two shells caused by shrinkage of the polymer liner, Moore (1998). The nonlinear buckling solution of Glock (1977) matches the trend of the data (at almost a slope of 2.2 on this log-log plot), and does not need artificial magnitude increase to be close to the measured pressures, though the tests were performed on liners clamped at the ends to external cylinders with length to diameter ratio L/D of 4, and end effects resulted in somewhat higher critical pressures despite the effect of imperfections, Moore (1998).

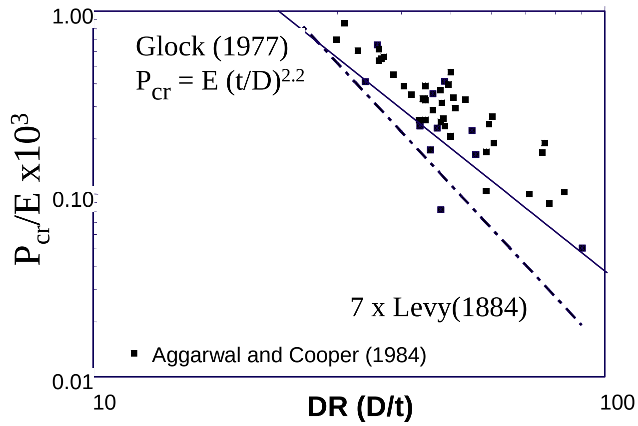

Figure 10. Test data of Aggarwal and Cooper (1984) versus calculations based on linear and nonlinear buckling theory.

3.3 *Finite element analyses of buckling strength and design considering imperfections*

An assessment of typical sewers requiring liners and the characteristics of the different liner processes lead El Sawy and Moore (1997) to consider systematic and characteristic imperfections of three different kinds (Figure 11):

a. oval shape (where $D_H \neq D_V$ due to the initial or fractured sewer geometry)
b. initial gap *d* between the external surface of the inner polymer shell and the inner surface of the rigid sewer
c. initial waviness in the liner of amplitude Δ (e.g. where the liner passes over a fracture or other longitudinal feature).

El Sawy and Moore (1997) used nonlinear finite element analyses of these three different geometrical issues to develop reduction factors R_q, R_Δ, and R_d to aid in calculating buckling pressures. For example, critical pressure for close fitting liners is

$$P_b = 1.0 E_{liner} \left(\frac{t_{liner}}{D_{liner}}\right)^{2.2} R_q R_\Delta \qquad [3]$$

where the liner has effective modulus E_{liner}, thickness t_{liner}, diameter D_{liner}, and R_q and R_Δ are correction factors used to account for pipe ovality *q* defined as

$$q = \frac{D_H - D_V}{D_H + D_V} \approx \frac{\Delta D_H}{ID_{pipe}} \qquad [4]$$

and small wavy imperfections.

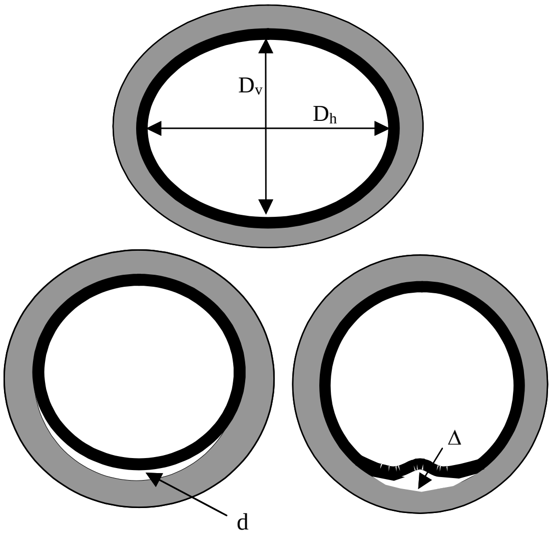

Figure 11. Oval, gap, and wavy liner imperfections.

If the liner drapes over a fractured rigid sewer at the invert, wavy imperfection amplitude Δ is given by

$$\Delta \approx 0.5 ID_{pipe} \left(\frac{\Delta D_H}{ID_{pipe}}\right)^2 \left(1 + \frac{2t_{pipe}}{ID_{pipe}}\right)^{-1} \qquad [5]$$

where ID_{pipe} is the internal diameter of the uncracked sewer. The expressions for reduction factors quantified by El Sawy and Moore (1997)

$$R_q R_\Delta = e^{-q/0.18} e^{-0.56\Delta/t_{liner}} = e^{-\Delta D_H/0.18 ID_{pipe}} e^{-0.28\frac{ID_{pipe}}{t_{liner}}\left(\frac{\Delta D_H}{ID_{pipe}}\right)^2} \qquad [6]$$

can then be used to estimate the magnitude of reduction in resistance to external fluid pressure (see Moore, 2008 for further details).

3.4 *Explanation of earth load effects and design for local bending*

The last decade has seen much debate concerning the potential effect of earth loads on liners placed within damaged sewers (e.g. Law and Moore, 2003). Influenced by the importance of buckling under external fluid loading, the standards have considered buckling resistance of the polymer liner to earth loads as well (in the absence of any other performance limit established as being important), and have used buried pipe buckling theory as though the structure were buried directly in the surrounding soil (e.g. ASTM F1216-93).

Law and Moore (2003) therefore conducted tests to examine interaction between the liner, the old sewer, and the surrounding soil, Figure 12. They demonstrated that the compressive hoop thrusts associated with earth loads are carried by the segments of old sewer (provided these remain in contact), and that it is not buckling under thrust but tensile stresses caused by local bending that need to be considered during design, Figure 13. Since the liner has a negligible effect on the stiffness of the repaired pipe system (deformations are primarily resisted by the surrounding ground), the strains in the liner can be effectively calculated using the solution for a ring under parallel plate loading subjected to diameter decrease ΔD_V:

$$\varepsilon_{cr} = \varepsilon_{in} = \pm \frac{\Delta D_v c}{2\pi \bar{R}_{liner}^2 \left(\frac{\pi}{8} - \frac{1}{\pi}\right)} = \pm \frac{2.139 \Delta D_v c}{\bar{R}_{liner}^2} \qquad [7]$$

where the liner has mid-surface radius of R_{liner}, and c is the distance from the liner mid-surface to the extreme fibre responding in tension (half the thickness for plain liners). Here, change in vertical pipe diameter ΔD_v is assumed to take place in some sections of the sewer after the liner is inserted. The value of ΔD_v determined from a CCTV inspection of the deformed pipe prior to lining should be used if, at the time of liner construction, there is a possibility of similar amounts of soil deterioration behind segments of unfractured pipe, Moore (2008). Finite element analysis of the problem supports the efficacy of this design approach, Law and Moore (2007), since strains calculated using [7] match both the finite element results and the measured strains, Figure 14.

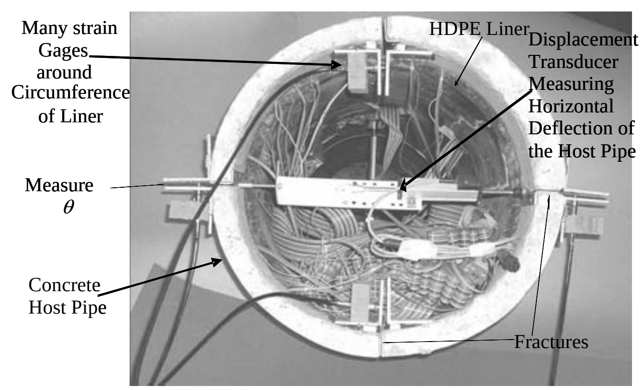

Figure 12. Sample for liner-host pipe-soil test, Law and Moore (2003).

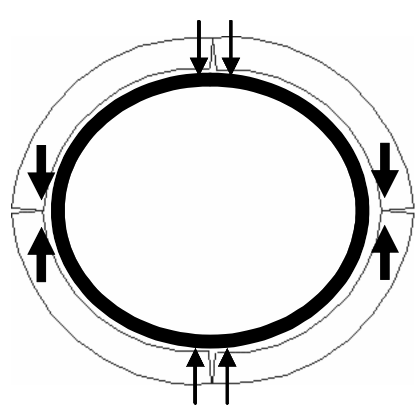

Figure 13. Thrusts pass through segments of the old sewer; local bending at liner crown and invert (Law and Moore, 2003).

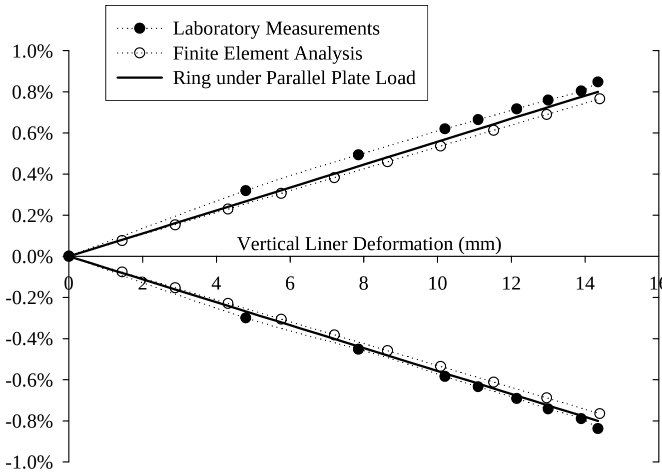

Figure 14. Design and computer calculations of local bending strain versus measurements, Law and Moore (2007).

4 PIPE REPLACEMENT USING BURSTING

Pipe bursting is a 30 year old technology where a conical expander is pulled through an old pipe to break it into fragments, push these aside, and pull a new (usually HDPE) pipe into place, Figure 15.

Medium and large scale laboratory tests at Queen's (e.g. Figure 16, Cholewa et al. 2008) have been used to develop data on the associated surface movements (e.g. Figure 17) and pulling forces (Lapos et al. 2004), for evaluation of computer models and evaluation of the parametric solutions that have then followed (Nkemitag and Moore, 2006, 2007).

a. Pipe bursting equipment in use in Ottawa, Ontario

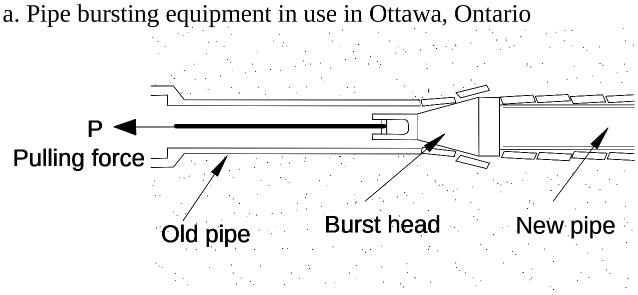

b. The pipe bursting process, Nkemitag and Moore, (2007).
Figure 15. Pipe replacement by static pipe bursting.

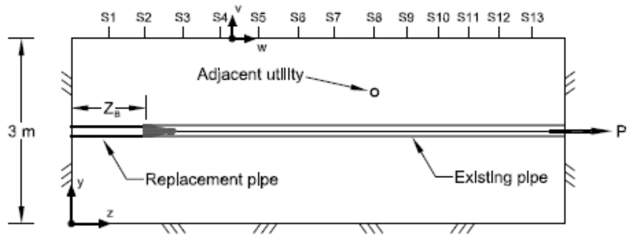

a. Test pipes and their locations.

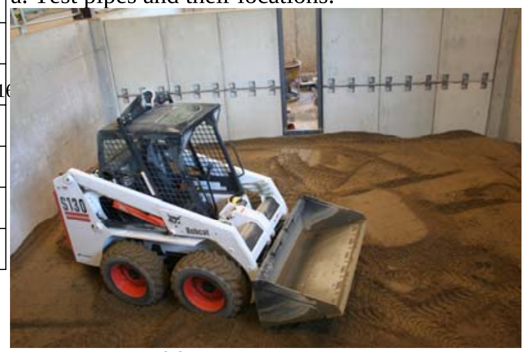

b. Placement of foundation soil.

c. Concrete sewer d. Adjacent PVC water pipe
Figure 16. Pipe bursting test, Cholewa et al. (2008).

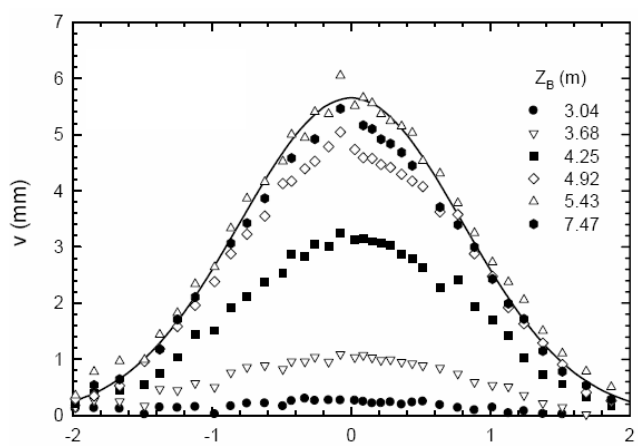

Figure 17. Surface uplift, Cholewa et al. (2008).

While British Gas developed and used 'proximity charts' for protection of infrastructure in the vicinity of pipe bursting operations (see Chapman and Rogers, 1991), further design procedures are now being developed to allow geotechnical and other consultants to directly estimate the response of the adjacent pipeline, Cholewa et al. (2008).

Figure 18 reports on finite element calculations of surface uplift during static pipe bursting in dense sand, Nkemitag and Moore (2006). A key to the analysis is correct treatment of the internal boundary, which needs to left free to move upwards and maintain vertical force equilibrium. Fernando and Moore (2002) proposed use of a high stiffness ring under internal pressure for this purpose, Figure 18a. Figure 18b shows four measured values of surface uplift reported by Lapos et al. (2004) as well as finite element calculations. Maximum surface uplift normalized by the increased diameter ΔD for the soil cavity resulting from the action of the conical expander is plotted against the magnitude of that cavity expansion relative to initial diameter D_0. Results for three different burial depths h/D_0 are presented. The experimental data implies the calculations are reasonable estimates accounting for the effects of initial pipe geometry, expander geometry, and pipe burial depth. Further studies of static pipe bursting include the development of finite element procedures to calculate the pulling forces required as an aid in equipment selection, Nkemitag and Moore (2007).

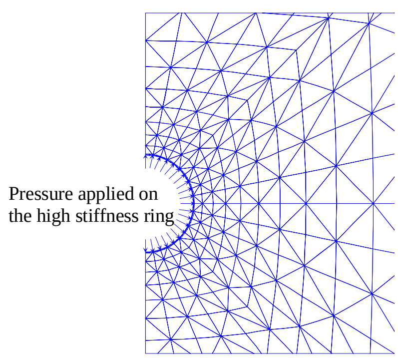

a. Treatment of internal boundary condition, Fernando and Moore (2002).

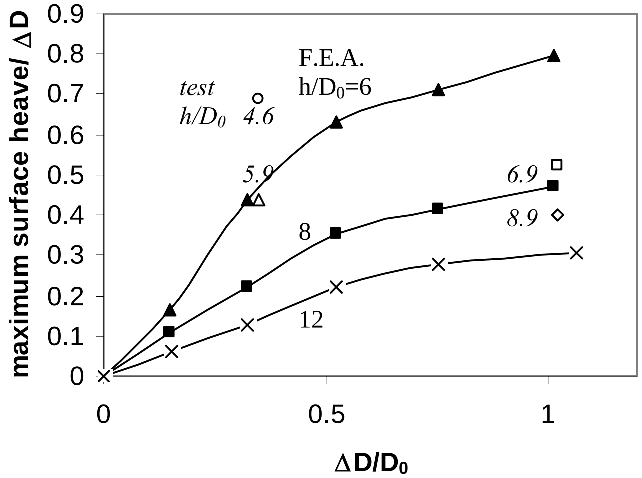

b. Uplift calculations for bursting in dense sand (Nkemitag and Moore, 2006) with the measurements of Lapos et al. (2004).
Figure 18. Finite element calculations of uplift.

5 INVESTIGATIONS OF HORIZONTAL DIRECTIONAL DRILLING

The fourth approach to pipe burial that is under examination is that of horizontal directional drilling. This procedure, common in North America and growing in importance elsewhere, involves drilling a preliminary borehole under the river or other obstruction being tackled, enlarging that hole using a reamer and pulling a new HDPE, steel or other pipe into place, Figure 19. Typically the borehole is stabilised with drilling mud, which is also used to lubricate the pipe and return soil cuttings to the ground surface.

Recent work includes the development of a soil-pipe interaction model to permit calculation of pulling forces on polymer or steel pipes being installed, Chehab and Moore (2008). Figure 20 shows calculations of axial force distribution at the end of installation, immediately thereafter, and over time as the ends are released, where the HDPE pipe is allowed a period of length (viscoelastic strain) recovery before it is tied to the objects it is connecting. This work first required extensions to the viscoelastic and viscoplastic models of Zhang and Moore (1997) for HDPE to permit successful calculation of strain reversal, then detailed consideration of the drag associated with movement of the pipe along the ground surface, through straight and curved sections of the borehole, as well as the drag induced by the viscosity of the drilling mud as it flows past the pipe.

Another important issue during drilling projects is the potential loss of drilling mud if the soil fails by either blowout, Figure 21a, or hydrofracture, Figure 21b. Computer modelling (Kennedy et al. 2007) and new closed form solutions (Xia and Moore 2006) have been developed to quantify the stress conditions under which these two mechanisms govern, and to extend existing cavity expansion solutions (e.g. Arends et al. 2003) to include the effect of coefficient of lateral earth pressure and produce more accurate (less unconservative) calculations of maximum allowable mud pressure, Figure 22.

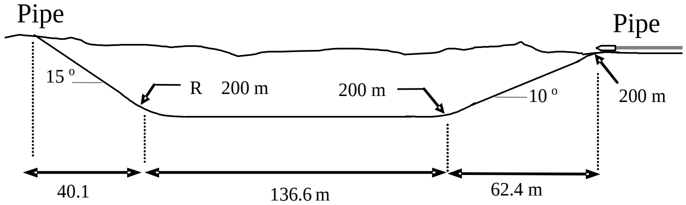

Figure 19. Dimensions of an example river crossing using directional drilling, Chehab and Moore (2008).

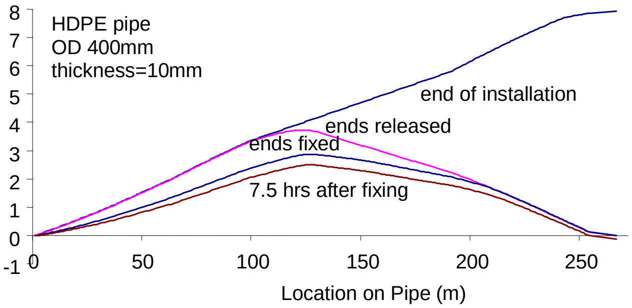

Figure 20. Axial force stress distributions calculated along the HDPE pipe at various times, Chehab and Moore (2008).

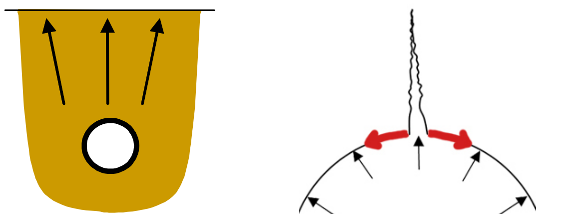

a. Blowout (plastic flow) b. Hydrofracture (tensile fracture)

Figure 21. Mud loss mechanisms, Kennedy et al. (2007)

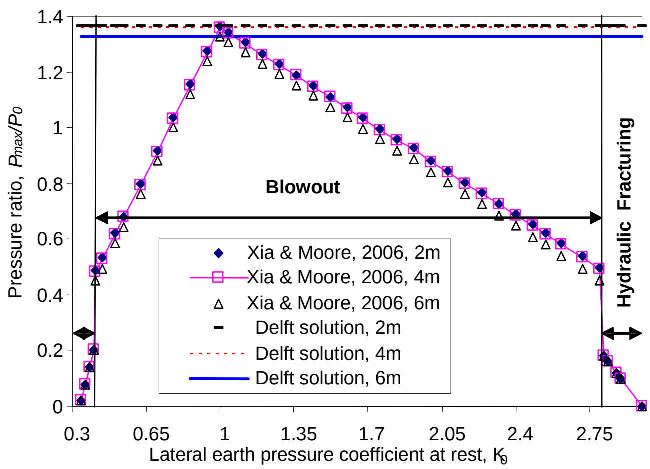

Figure 22. Maximum mud pressure as a function of K_0, cohesive soil with c_u/σ_v=0.1, Xia and Moore (2006).

6 ACKNOWLEDGEMENTS

Firstly, my sincere thanks to Michael for shared learning experiences regarding shells and shell-solid interaction, and many enjoyable drives discussing life and engineering mechanics.

The work reported here was supported by the Natural Sciences and Engineering Research Council of Canada, the Canada Foundation for Innovation, and various other industrial and government sponsors. The contributions to this work of colleagues Richard Brachman, Kerry Rowe, and Andy Take and current and former graduate students Abdul Chehab, John Cholewa, Khaled El Sawy, Mohamed El Taher, Viji Fernando, Matt Kennedy, Brian Lapos, Michael Law, Michael Nkemitag, Zheng Tan, Hongwei Xia, and Charles Zhang are gratefully acknowledged.

7 REFERENCES

Aggarwal S.C. & Cooper, M.J. 1984 External pressure testing of Insituform lining, Internal report, Coventry Polytechnic

Arends, G. 2003 Need & possibilities for a quality push within the technique of hor.dir.drill. No-Dig 2003, Las Vegas.

ASTM F1216 1993 Standard practice for rehab. of existing pipelines & conduits by the inversion and curing of a resin-impregnated tube, ASTM Int., West Conshohocken, PA.

Chapman D.N. & Rogers C.D.F. 1991 Ground movements associated with trenchless pipelaying operations, 4th Intl. Conf. on Gr. Mov & Struc. , Cardiff, Pentech Press, 91-107.

Chehab, A.G. & Moore, I.D. 2008. 2008. Polymer pipes in trenchless applications: HDPE pipe response during pulled in place installation, Geoamericas 2008, Cancun, Mexico.

Cholewa, J.A, Moore, I.D. & Brachman, R.W. 2008., Response of a PVC water pipe during concrete sewer replacement by bursting, NASTT 2008 No-Dig Conf, Dallas, E-3-04, 8pp.

El Sawy, K. & Moore, I.D., 1997. Param.study for buckling of liners: effect of liner geom.& imp. Boston ASCE 416-423.

El Taher, M. & Moore, I.D. 2008. Finite element study of corroded metal culvert stability, (to appear, Transp.Res.Rec.).

Fernando, V. & Moore, I.D. 2002. Use of cavity expansion theory to predict ground displacement during pipe bursting, Pipelines 2002, ASCE, Cleveland,11pp.

Hoeg, K. 1968. Stresses against underground structural cylinders, J. Soil Mech& Fnd.Eng, ASCE, 94, (4), 833-858.

Glock, D., 1977 Uberkritisches verhalten eines starr ummautelten kriesrohres bei wasserdruck von auβen und temperaturdehnung; Der Stahlbau, 7, 212-217.

Kennedy, M. Skinner, G. & Moore, I.D. 2007 Limiting drilling slurry pressures to control hydr. fracturing during directional drilling operatns in purely cohesive soil, TRR. 1976, 172-180.

Lapos, B., Brachman, R.W.I & Moore, I.D. 2004 Laboratory measurements of pulling force & ground movement during a pipe bursting test. No-Dig 2004. New Orleans, B-1-04.

Law, T.C.M & Moore, I.D. 2003 Behaviour & design of sewer liners for earth load, Int. No-Dig., Las Vegas, 15pp.

Law, T.C.M. & Moore, I.D. 2007. Numerical modeling of tight fitting flexible liner in damaged sewer under earth loads, Tun. & Undergr. Space Tech., 22, 655–665.

Levy, M. 1884 Me'memoire sur un nouveau cas inte'grable du proble'm de l'elastique et l'une de ses applications, J. Math. Pure et Appl., (Lioville), Series 3, 10, 5-42.

Marston, A. & Anderson, A.O. 1913 The theory of loads on pipes in ditches and tests on cement and clay drain, tile and sewer pipe, Eng. Exp. Stn, Iowa State College, Bulletin 31.

Moore, I.D. & El-Sawy, K., 1996. Buckling strength of polymer liners used in sewer rehab..Tr.ResRec 1541 127-132.

Moore, I.D., 1998. Tests for pipe liner stability: What we can and cannot learn. No-Dig '98, Albuquerque, 444-457.

Moore, I.D. 2008. Sewer & culvert deterioration & its implications for design of liners. Keynote, Tr, Aus., Sydney, 12pp.

Nkemitag, M. & Moore, I.D. 2006 Rational guidelines for expected ground disturbance during static pipe bursting through sand, Paper E-2-01, No-Dig 2006, Nashville, 9pp.

Nkemitag, M. & Moore, I.D. 2007 Longit. progr. burst head dur.pipe burstg: cal. pull. forces. Tr.Res.Rec.1018 203-210.

Spangler, M.J. 1956, Stresses in pressure pipelines and protective casing pipes, J. Str,Eng., ASCE, 82, 1-33.

Spasojevic, A. Mair, R.J. & Gumbel, J.E.2007 Centrifuge mod. effects of soil loading flex. sewer liners, Géot. 57 331-341.

Tan, Z. & Moore, I.D. 2007 Effect of backfill erosion on moments in buried rigid pipes, TRB Conf, Wash. 29pp.

Xia, H. & Moore, I.D. 2006. Estimation of max. mud pressure in purely cohesive mat. dur. dir.drill., Geom& GeoEng, 1, 3-11.

Zhang, C.& Moore, I.D. 1997. Nonl. Mech. response HDPE: Part II-Uniaxial const. mode. J. Pol.Eng.& Sc. 37, 414-420.